Supplemental red LED light promotes plant productivity, "photomodulate" fruit quality and increases *Botrytis cinerea* tolerance in strawberry

Giulia Lauria[a], Ermes Lo Piccolo[a], Costanza Ceccanti[a,b,*], Lucia Guidi[a,b,c], Rodolfo Bernardi[a,b], Fabrizio Araniti[d], Lorenzo Cotrozzi[a,b], Elisa Pellegrini[a,b], Michela Moriconi[a], Tommaso Giordani[a,b], Claudio Pugliesi[a], Cristina Nali[a,b,c], Luigi Sanità di Toppi[e], Luca Paoli[e,], Fernando Malorgio[a,b], Paolo Vernieri[a,b], Rossano Massai[a,b], Damiano Remorini[a,b], Marco Landi[a,b]

[a] *Department of Agriculture, Food and Environment, University of Pisa, Via del Borghetto, 80 - 56124 Pisa, Italy*

[b] *Interdepartmental Research Center Nutrafood "Nutraceuticals and Food for Health", University of Pisa, Via del Borghetto, 80 - 56124 Pisa, Italy*

[c] *CISUP, Centre for Instrumentation Sharing, University of Pisa, Largo Bruno Pontecorvo, 3 - 56127 Pisa, Italy*

[d] *Department of Agricultural and Environmental Sciences - Production, Landscape, Agroenergy, University of Milan, Via Celoria, 2 - 20133 Milan, Italy*

[e] *Department of Biology, University of Pisa, via Luca Ghini, 13 - 56126 Pisa, Italy*

* *Correspondence*: costanza.ceccanti@agr.unipi.it

Abstract

This work provides new evidences on the effect of pre-harvest red (R), green (G), blue (B), and white (W – R:G:B; 1:1:1) LED light supplementation on production, nutraceutical quality and *Botrytis cinerea* control of harvested strawberry fruit. Yield, fruit colour, firmness, soluble solid content, titratable acidity, primary and specialized metabolites, expression of targeted genes and mould development were analyzed in fruit from light-supplemented plants, starting from the strawberry flowering , radiating 250 μmol m^{-2} s^{-1} of light for five hours per day (from 11:00 to 16:00 h), until the fruit harvest. Briefly, R light induced the highest productivity and targeted anthocyanin accumulation, whilst B and G lights increased the accumulation of primary and secondary metabolites especially belonging to ellagitannin and proanthocyanidin classes. R light also promoted pathogen tolerance in fruit by the upregulation of genes involved in cell wall development (*F×aPE41*), inhibition of fungus polygalacturonases (*F×aPGIP1*) and the degradation of *B. cinerea* beta-glucans (*F×aBG2-1*). Our dataset highlights the possibility to use red LED light to increase fruit yield, "photomodulate" strawberry fruit quality and increase *B. cinerea* tolerance. These results can be useful in terms of future reduction of agrochemical inputs throught the use of R light, enhancing, at the same time, fruit production and quality. Finally, further analyses might clarify the effect of pre-harvest supplemental G light on postharvest fruit quality.

Keywords: Anthocyanins; *Fragaria* × *ananassa*; Light eustress; Secondary metabolism; Pathogen; Priming effect

1. Introduction

Light is one of the most important environmental factors for plant growth, development, and fruit quality. The utilization of appropriate lighting parameters (i.e., intensity, photoperiod, and spectral quality) can regulate and enhance plant and fruit cell function, appearance and production of metabolites in food crops, especially in indoor cultivations (Lauria et al., 2021). Nowadays, light emitting diodes (LEDs) have gained popularity due to their energy-saving, cheaper and compact nature than traditional light sources (i.e., fluorescent, filament and high-pressure sodium lamps; Al Murad et al., 2021). At the same time, the LEDs narrow spectrum can provide specific wavelengths to match photoreceptors (Lin et al., 2013), revolutionizing horticultural crop production, preservation, and protection against pathogen challenge.

Strawberry (*Fragaria* × *ananassa* Duch.) is a fruit crop widely cultivated in the Mediterranean regions due to its sweet taste and various nutritional benefits. In terms of bioactive compounds, ordinary ripening process under natural conditions results in the increase of hydroxycinnamic and hydroxybenzoic acids, flavonoids (especially quercetin and kaempferol glycosides), anthocyanins (as pelargonidin and cyanidin glycosides) as well as hydrolysable and condensed tannins contents (Aaby et al., 2012). The complexity of the specialized metabolic profile in strawberry fruit is a well-appreciated feature in view of the proven antioxidant activity of several of these compounds and therefore their possible contribution to the containment of the infection caused by typical and widespread strawberry pathogens such as the ubiquitous necrotrophic fungus *Botrytis cinerea* causing grey mould (Petrasch et al., 2019).

The perishable nature of strawberry fruit, due to their low firmness, and the frequent development of grey mold caused by *B. cinerea* limit fruit quality as well as their shelf life and marketability (Petrasch et al., 2019). The use of monochromatic LEDs to improve the fruit quality was previously studied in strawberry, peach, banana, and other fruit during postharvest storage (Huang et al., 2018, Kim et al., 2011). Results showed the accumulation of ascorbic acid, total phenols

and total sugars in banana fruit exposed to blue (464–474 nm), red (617–627 nm) and green (515–525 nm) LED light with the photosynthetic photon flux densities of approximately 3920, 4340 and 5200 µmol photon m^{-2} s^{-1}, with an acceleration of banana ripening under blue light exposure (Huang et al., 2018). Kim et al. (2011) observed an increase in anthocyanin content in strawberry fruit subjected to red, blue and green LEDs in postharvest and an increment in ascorbic acid content when fruit were exposed to blue light. The same blue light induced an increase of phenolic compounds in strawberry fruit, while total soluble solids accumulation was improved by postharvest exposure to green light (Kim et al., 2011).

Conversely, few works utilize fully-monochromatic LED light environments and even fewer works are available on the use of supplemented monochromatic LED light (i.e., LED enrichment of ambiental light in greenhouse experiments) during plant cultivation to improve fruit yield, quality, and tolerance to pathogen attack (Choi et al., 2015; Ngcobo et al., 2020). For example, Ngcobo et al. (2020) observed an increase of lycopene content in tomato fruit treated with fully monochromatic red LED light (peak at 634 nm, 120 ± 20 µmol m^{-2} s^{-1}) or blue LED light (peak at 450 nm, 120 ± 20 µmol m^{-2} s^{-1}) for 8 h per day for seven consecutive days. Choi et al. (2015) showed a remarkably higher production of strawberry fruit when the greenhouse ambient light was supplemented with either blue LED light (peak at 448 nm) or with the combination of blue and red LED light (peak of red light at 634 and 661 nm and ratio blue:red =3:7) for 6 hours per day for 151 days. Regarding the tolerance to pathogen attack, Gallé et al. (2021) reviewed the defense mechanisms activated by plants under red light exposure to cope with pathogens, reporting a regulation of the Reactive Oxygen Species (ROS) metabolism and the redox homeostasis, as well as the contribution to the biosynthesis and activation of defense-related phytohormones (e.g., salycilic acid, jasmonate and ethylene).

The present work aimed to evaluate the effect of monochromatic red (R), green (G), blue (B) and polychromatic (W– R:G:B, 1:1:1) LED light supplementation on strawberry fruit production, organoleptic quality, accumulation of primary and secondary metabolites and postharvest tolerance to *B. cinerea* infection.

2. Materials and Methods

2.1 Plant material, growing conditions, and fruit yield measurement

Cold-stored strawberry plantlets (*F.* × *ananassa* var. Elsanta) at –2 °C were purchased by COVIRO srl (Cervia, RA, Italy). Fifty plantlets (ten for each treatment) were transplanted on April 19th, 2021 into a glasshouse located at the Department of Agriculture, Food and Environment (DAFE), University of Pisa (43,704672°N, 10,427292°E). Each plant was hydroponically cultivated in a substrate with a coarse and draining structure composed of chopped blonde peat, Irish peat, coconut fiber and perlite (X-BAG P30, Virgoplant Italia srl, Fombio, LO, Italy) characterized by pH 5.5-6.5, electrical conductivity (EC) 0.15-0.25 dS m^{-1}, total porosity 90 % and fertilized by water-soluble NPK fertilizer and 500 g m^{-2} microelements. The average of growing conditions were: 25.9 °C mean temperature, 52 % humidity and 434 µmol m^{-2} s^{-1} daily mean solar light radiation. All plants were fed with a nutrient solution optimized in a previous study for strawberry fruit growth (Lauria et al., 2021) with minor modifications and containing N-NO_3^- 10.0 mM, N-NH_4^+ 1.0 mM, P-PO_4^{3-} 1.0 mM, K^+ 6.5 mM, Ca^{2+} 5.2 mM, Mg^{2+} 1.2 mM, S-SO_4^{2-} 4.2 mM, Fe^{2+} 20.0 µM, BO^{3-} 30.0 µM, Cu^{2+} 1.0 µM, Zn^{2+} 5.0 µM, Mn^{2+} 10.0 µM, Mo^{3+} 1.0 µM; EC and pH were 2.25 dS m^{-1} and 5.6, respectively. These latter parameters were checked daily and adjusted to keep them within 10 % of the values measured in the fresh nutrient solution. Daily fertigation was used during the first month of the experiment, whereas, in the second month, it was supplied twice a day through drip irrigation. The supplementation of LED lights (Ambra Elettronica srl, Bolzano Vicentino, VI, Italy) started on May 3rd, 2021 (starting from the strawberry flowering) , radiating 250 µmol m^{-2} s^{-1} of light for five hours per day (from 11:00 to 16:00 h) until the fruit harvest. Control (NS) plants were shadowed to simulate the shadow condition of the other treatments caused by the physical presence of lamps, while, for the LEDs supplementation, plants were exposed to environmental light supplemented by

117 red (R; peak 660 nm), blue (B; 450 nm), green (G; 520 nm), and polychromatic (W – R:G:B, 1:1:1)
118 LED lights (Supplementary material, Fig. S1).

119 Strawberry fruits were harvested at the commercial stage, ensuring that fruit from different
120 treatments had reached similar ripening level (75-90 % red). All the fruit were weighted to evaluate
121 the overall productivity and then fruit were arranged in four sub-samples for each treatment, each
122 showing homogeneous and representative features. The first sub-sample was used for the organoleptic
123 analyses at harvest time, and the second one was freeze-dried until the plant material reached a
124 constant weight. The third sub-sample was frozen in liquid nitrogen and stored at –80 °C until
125 biochemical analyses. Finally the fourth sub-sample of fruit was used for *B. cinerea* fruit inoculation
126 and gene expression analysis.

127 *2.2 Fruit color, firmness, soluble solid content and titratable acidity*

128 Fruit color measurements were carried out by a Konica Minolta CM-700d colorimeter
129 (Minolta, Osaka, Japan) in the CIE mode L*, a*, and b*, in which L* (lightness) is the coordinate of
130 brightness (z axis), which ranges from –100 (black) to +100 (white); a* is the hue coordinate (x axis),
131 which ranges from +60 (red) to –60 (green); b* is the hue coordinate (y axis), which ranges from +60
132 (yellow) to –60 (blue). The chromameter was calibrated with a standard white tile.

133 Fruit firmness was measured by loading strawberry fruit on a Turoni penetrometer, model
134 53205 (T.R. Turoni, Forlì, FC, Italy). Each sample was placed stationary on a stand and the
135 compressive force (N) required for 5 mm deformation of the fruit was recorded. Then, each fruit
136 under analysis was homogenized in a mortar to obtain fruit juice for soluble solid content (SSC) and
137 titratable acidity (TA) analysis. The SSC was measured using a digital refractometer (Atago, Tokyo,
138 Japan) and expressed as %. Then, 1 g of fruit flesh diluted with 30 mL distilled H_2O was titrated with
139 0.1 N NaOH until reaching pH 8. For TA determination, TA was expressed as citric acid %. All
140 analyses were carried out considering 20 replicates per treatment.

141 *2.3 GC–MS-driven untargeted metabolomics analysis*

142 Analyses were performed in freeze-dried fruit belonging to the second sub-sample (section
143 2.1). Sample extraction, derivatization and analysis were performed according to Landi et al. (2020a).
144 The analysis was carried out using an Agilent gas chromatography apparatus (7890A) equipped with
145 a single quadrupole mass spectrometer (5975C Inert XL MSD, Agilent Technologies, Santa Clara,
146 U.S.A.). A standard volume (1 µl) for each sample was injected into a capillary column in arrow-free
147 mode (MEGA-5 MS, 30 m × 0.25 mm × 0.25 µm + 10 m of pre-column; MEGA, Legnano, Italy).
148 Injector and source temperature were settled at 250 °C and 260 °C, respectively, and the following
149 temperatures were used to analyzed samples: isothermal at 70 °C for 5 min followed by a 5 °C min^{-1}
150 ramp until 350 °C and a final 5 min heating at 330 °C. Mass spectra were registered in Electronic
151 Impact (EI) mode at 70 eV, scanning in the range 40–600 *m/z*, scanning for 0.2 s. Solvent delay by
152 mass spectrometry has been set at 9 min. Instrumental performance, tentative identification and the
153 monitorage of shifts in retention indices were guarded injecting n-Alkane standards (C10–C40 all
154 even) and blank solvents at programmed intervals.

155 *2.4 Extraction of polyphenols and anthocyanins for UHPLC-HR-ESI-MS analysis*

156 Polyphenols were extracted from fresh strawberry fruit with 80 % (*v/v*) ethanolic aqueous
157 solution (3 g in 10 mL) from fruit belonging to the third sub-sample (section 2.1). Each extract was
158 sonicated for 20 min by a sonicator (Digital ultrasonic Cleaner, DU-45, Argo-Lab, Modena, Italy)
159 and then centrifuged through a centrifuge (MPW-260R, MWP Med. Instruments, Warsaw, Poland)
160 for 5 min at 4000 × g.

161 Anthocyanins were extracted from fresh strawberry samples with 2 % methanol/hydrochloric
162 acid mixture (1 g in 6 mL) for 15 min under stirring, then samples were centrifuged for 5 min at 4000
163 × g. The supernatants of both extractions were injected into the LC-MS system.

164 *2.5 UHPLC-HR-ESI-MS analysis*

165 The phenolic composition of strawberry extracts was investigated using ultra-high-
166 performance liquid chromatography (UHPLC) coupled with a high resolution-mass spectrometer

(HR-MS). The extracts were centrifuged (4000 × g) and injected (5 µL) into the LC-MS system, composed of a Vanquish Flex Binary UHPLC system and a Q Exactive Plus MS Orbitrap-based FT-MS system equipped with an electrospray ionization (ESI) source (Thermo Fischer Scientific Inc., Bremem, Germany). The analysis of all phenols was performed on a Kinetex® EVO C18 column (100 × 2.1 mm, 2.6 µm) provided by a SecurityGuard™ Ultra Cartridges (Phenomenex, Bologna, Italy), eluting with a mixture of formic acid in acetonitrile 0.1 % (*v/v*; solvent A) and formic acid in water 0.1 % (*v/v*; solvent B) at a flow rate 0.5 mL min^{-1}, using the following solvent gradient: 5 % A, 0-2 min; 5 to 80 % B, 2-32 min. The analysis of anthocyanins was performed on a Kinetex® Biphenyl column (100 × 2.1 mm, 2.6 µm) provided by a SecurityGuard™ Ultra Cartridges (Phenomenex, Bologna, Italy) eluting with the same mixture of formic acid (solvent A) in acetonitrile and formic acid in water (solvent B) as described for the phenol analysis but, in this case, a linear solvent gradient of increasing 10 to 35 % solvent A within 5 min was developed. The autosampler and column oven temperature was maintained at 4 and 35 °C, respectively. The ESI interface was used in negative ion mode to analyze phenols and positive ion mode for anthocyanins. Mass spectra were acquired in a scan range of *m/z* 200-2000 for phenols and *m/z* 250-1200 for anthocyanins operating in full (70,000 resolution, 220 ms maximum injection time) and data dependent MS/MS scan (17,500 resolution, 60 ms maximum injection time). Ionization parameters were optimized as follows: nebulization voltage 3500 V, capillary temperature 300 °C, sheath gas (N_2) 20 arbitrary units, auxiliary gas (N_2) 3 arbitrary units, HCD (Higher-energy C- trap dissociation) 18 eV. Data acquisition and processing were achieved with the Xcalibur® data system (Thermo Scientific, San Jose, CA, USA). All compounds were tentatively identified by comparison of their elution order, HR full mass spectra and fragmentation patterns (MS/MS) with literature data, considering an accepted mass error < 5 ppm.

2.6. Botrytis cinerea inoculum preparation and fruit inoculation

191 *Botrytis cinerea* (isolate 8335), initially isolated from infected strawberry fruit and preserved
192 in the DAFE-culture collection, was cultured in Petri dishes on potato dextrose agar (PDA, 39 g L^{-1},
193 Sigma-Aldrich, Milan, Italy) amended with streptomycin sulphate (0.1 g L^{-1}, Gold Biotechnology,
194 Saint Louis, MO, USA), at 23 ± 2 °C under a photoperiod of 12 h.

195 A conidial suspension of *B. cinerea* was prepared from a static 15-day-old culture in
196 Erlenmeyer flasks (0.25 L) containing potato dextrose broth (PDB, 20 g L^{-1}, Sigma-Aldrich, Milan,
197 Italy). After two days at 23 °C, the conidia concentration of the suspension was adjusted to
198 approximately 1×10^5 mL^{-1} by a Bürker hemacytometer chamber (Henneberg-Sander, Giessen-
199 Lützellinden, Germany). Fruit of a fifth subset (section 2.1) were inoculated by dropping 10 µL of
200 the conidial suspension on the fruit surface toward the base (Haile et al., 2019). The same procedure
201 was followed for the control treatment, where distilled sterilized water was used instead (not
202 inoculated). After treatments, fruit were maintained in clear and unsealed plastic chambers
203 (inoculated and control fruit were kept separated) under natural light and temperature conditions, and
204 in high humidity (provided by wet sterile paper towels placed in the chambers without touching the
205 fruit).

206 *2.7. Assessment of disease development*

207 Disease severity was calculated every 12 h using an ordinal 1-6 rating system: 1 = no
208 symptoms; 2 = symptom onset; 3 = necrotic lesions without mycelium; 4 = < 33 % of fruit surface
209 covered by mycelium; 5 = 33-66 % of fruit surface covered by mycelium; 6 = > 66 % of fruit surface
210 covered by mycelium. The Area Under the Disease Progress Curve (AUDPC) was determined using
211 the formula reported in Simko and Piepho (2012):

212 $$AUDPC = \sum_{i=1}^{n-1} \frac{y_i + y_{i+1}}{2} \times (t_{i+1} - t_i)$$

213 where y_i is the rate of disease severity determined as described above at the i^{th} observation, t_i
214 is time (in hours) at the i^{th} observation, and n is the total number of observations.

2.8. Gene expression analysis by quantitative real-time polymerase chain reaction (qRT-PCR)

The expression of some genes known to be involved in molecular response to *B. cinerea* infection was analysed. Total RNA was extracted from 700 mg of non-inoculated and *B. cinerea*-inoculated fresh fruit tissues of *F.* × *ananassa* plants grown under R light and NS treatments. Gene expression was determined after 24 and 48 h post-inoculation (hpi). Total RNA was extracted using cethyltrimethylammonium bromide (CTAB) method as described by Natali et al. (2018) with minor modifications. Fruit samples were homogenised in liquid nitrogen and incubated at 60 °C for 5 min in 2 mL extraction buffer [CTAB 2 % *w/v*, polyvinylpyrrolidone (PVP) 2 % *w/v*, Tris-HCl 300mM pH 8, ethylenediaminetetraacetic acid (EDTA) 25mM, NaCl 2.5 M, β-mercaptoethanol 2 % *v/v*]. Then, samples were extracted twice with an equal volume of chloroform:isoamyl alchol (24:1) and nucleic acids were precipitated by adding 3 M Na-acetate and cold isopropanol (1:6 *v/v*). Samples were centrifuged at 8000 × *g* for 30 min at 4 °C. The pellets of nucleic acids were washed with aqueous ethanol (70 % *v/v*) and solubilised in Tris-EDTA buffer. A DNAse I (Roche, Mannheim, Germany) treatment was utilised to remove genomic DNA contamination. Finally, RNAs were purified by phenol/chloroform extraction (1:1 *v/v*) and precipitated following standard procedures.

RNA purity and integration were checked through spectrophotometric and gel electrophoresis assays. The concentration of each RNA sample was measured using Qubit RNA BR Assay Kits (Invitrogen, Life Technology Corporation, Eugene, OR, USA). Afterwards, 400 ng of RNA samples were treated with Amplification Grade DNase I (Sigma-Aldrich) and reverse-transcribed into cDNA employing the Maxima First Strand cDNA Synthesis Kit (Thermo Fisher Scientific, Vilnius, Lithuania). The genes analyzed were: *Cynnamoil CoA reductase* (*F×aCCR1*), *Beta-1,3-glucanase* (*F×aBG2-1*), *Cellulose synthase-like protein D3* (*F×aCSLD3*), *Long-chain acyl-CoA synthetase 4* (*F×aLACS4*), *Lignin forming anionic peroxidase* (*F×aLFAP*), *Disease resistant protein RPM1-like* (*F×aRPM1*), *Polygalacturonase-inhibiting protein* (*F×aPGIP1*), *Pectate Lyase* (*F×aPECL*) and *Pectinesterase 41* (*F×aPE41*). The synthesized cDNA was used for quantitative real-time polymerase

chain reaction (qRT-PCR) using gene-specific primer pairs, as reported by Edger et al. (2019) and Lee et al. (2021b) (Supplementary material, Table S1). Real-time PCR was performed in the presence of Fast SYBR™ Green Master Mix (Applied Biosystems, Thermo Fisher Scientific, Vilnius, Lithuania), using a Real-time StepOnePlus™ apparatus (Applied Biosystem, Thermo Fisher Scientific Waltham, MA, USA). The thermal cycling conditions of RT-PCR were: reverse transcription: 48 °C for 30 min; activation: 95 °C for 10 min; cycling: 40 cycles 95 °C for 15 min/59 °C for 30 min; melt curve: 95 °C for 15 s/60 °C for 15 s/95 °C for 15 s. Here, *actin* (NCBI Reference Sequence: LC017712.1) and *Histone H4* (NCBI Reference Sequence: AB197150.1) were selected as housekeeping genes. Although both tested endogenous control genes exhibited adequate stable expression among the different samples, *Histone H4* was chosen to normalize gene expression data for its higher transcriptional stability compared to *actin*. The amplification of the target genes and the endogenous controls were run using at least three biological replicates, each with three technical replicates, and were analyzed on the same plate in separate tubes. The relative transcript abundance was calculated using the $2^{-\Delta\Delta C}$T method. Relative transcript values were calculated using uninfected fruit from plants grown under NS treatment as a reference sample. Before the quantification, a validation experiment was performed to ensure that amplification efficiencies of the target and reference genes were similar.

2.9. Statistical analysis

All data (± standard deviation; SD) from fruit yield, organoleptic analysis, UHPLC-HR-ESI-MS, AUDPC and qRT-PCR were analyzed by one-way analysis of variance (ANOVA), considering the supplementation with different LED lights as a source of variation. All the means were separated by Tukey's HSD (honestly significant difference) *post-hoc* test ($p \leq 0.05$). The normality of data was tested using Shapiro-Wilk test, whilst the homoscedasticity was tested using Bartlett's test. These statistical analyses were conducted using GraphPad (GraphPad, La Jolla, CA, USA). Transcript levels

of genes analyzed at 24 hpi did not show significant differences. For this reason, data are not shown in the manuscript.

Raw GC–MS data were analyzed using the software MS-Dial v.4.48 coupled with a purpose-built EI spectra library. The software parameters used for data collection, peak detection, deconvolution, alignment, and filtering were handled as reported in Fausto et al. (2021). Data annotation was carried out in MS-Dial using publicly available libraries. Identification of compounds was based on a comparison of the mass spectral pattern with EI spectral libraries, such as MoNA (Mass Bank of North America, http://mona.fiehnlab.ucdavis.edu/), MassBank, and the mass spectra and retention time index spectral libraries from the Golm Metabolome Database (Horai et al., 2010). Metabolite annotation and assignment of the EI-MS spectra were achieved following the guidelines for the metabolomics standards initiative for compounds identification; that is, level 2 (identification was based on a spectral database) and level 3 (only compound groups were known, i.e., specific ions and RT regions of metabolites; Sansone et al., 2007).

Experiments were carried out using a completely randomized design with three technical replications for each developmental stage. Metabolomics data were analyzed using the software Metaboanalyst 5.0 (Chong and Xia, 2020) and were normalized using the internal standard normalization functions in the MS-Dial software. The internal standard normalized data set was transformed through '$\log_2$ normalization' and Pareto scaled (Chong and Xia, 2020). The data were then classified through unsupervised multivariate principal component analysis (PCA). The output comprised score plots to visualize the contrast between different samples and loading plots to explain the cluster separation. Partial least-squares discriminant analysis (PLS-DA) was used to highlight differences among the metabolic phenotypes at five light treatments and to identify the metabolites mainly involved in groups separation and their change in concentration over time. To avoid overfitting, the PLS-DA model was validated using Q2 as a performance measure, the 10-fold cross-validation and setting, in the permutation test, a permutation number of 20 (see figures reported in Supplementary material, Table S2-plsda loadings).

290 Further, data were analyzed through the univariate ANOVA using Fisher's *post-hoc* least
291 significant difference test ($p \leq 0.05$ to highlight statistical differences among single metabolites and
292 light treatments; Supplementary material, Table S2-anova-posthoc). A false discovery rate was
293 applied to the nominal p-values as a control for false-positive findings. All the features significantly
294 affected by the treatments (in the ANOVA test) were presented as a heatmap and clusterized using
295 the Euclidean method for distance measurement and the Ward algorithm for groups clusterization.
296 Finally, all the metabolomic data were compared with control (NS *vs* W, NS *vs* G, NS *vs* B,
297 NS *vs* R) in the pathways analysis, which combines enrichment and topology analysis to highlight
298 the metabolic pathways affected by the different light spectra. As for the ANOVA analysis, a false
299 discovery rate was applied to the nominal p-values as a control for false-positive findings. All the raw
300 and analyzed metabolomic data are reported in Supplementary material, Table S2.
301

302 ## 3. Results

303 ### *3.1 Fruit yield and fruit organoleptic quality*

304 A higher fruit number was observed in plants supplemented with R light respect to NS, W and
305 B light. B and G light-exposed plants showed a significantly similar fruit number as detected in NS
306 plants (Fig. 1A). In terms of fruit weight, the R light supplementation showed the highest significant
307 value, followed by B light and NS, while G and W light supplementation revealed lower fruit weight
308 than R light (Fig. 1B).
309 Plants exposed to G lights showed higher lightness (L^*) values in fruit when compared with
310 the other treatments (Fig. 1C). Fruit redness index (a^*) was not affected by monochromatic LED light
311 supplementation, except for a slight significant decrease in fruit from plants under R light exposure
312 (Fig. 1D), whilst the yellowness index (b^*) was higher in control fruit and in fruit from plants
313 supplemented with G light (Fig. 1E).

314 The highest resistance to compressive force (compactness) was detected in fruit from G
315 supplemented plants, followed by fruit from R and W light supplemented plants (Fig. 1F). No
316 significant differences were reported in SSC of fruit from supplemented plants when compared with
317 control (Fig. 1G), whilst the highest TA values were observed in fruit from G and R treatments and
318 control plants (Fig. 1H).

319 *3.2. GC–MS-driven untargeted metabolomics analysis results*

320 The GC–MS–driven untargeted metabolomics analysis of LED–treated strawberry plants in
321 pre-harvest allows to annotate and quantify 87 metabolites, whereas 151 remained unknown
322 (Supplementary material, Table S2). Most of these annotated metabolites belonged to the primary
323 metabolism (amino acids, sugars, organic acids, nucleic acids, and fatty acids) and, to a lesser extent,
324 to plant specialized metabolites (e.g., epicatechin, N-methyl ethylamine). The one-way ANOVA
325 analysis revealed that 75 out of 88 metabolites were differentially produced among light treatments
326 (Supplementary material, Table S2). Results of this analysis were reported differentiating the
327 compounds in their chemical classes and, in particular, 35 organic acids, 17 sugars and 8 amino acids,
328 5 fatty acids and 1 nucleic acid were found in strawberry supplemented and control plants, whilst 8
329 molecules resulted from specialized metabolites (Fig. 2 and Supplementary material, Table S2). The
330 unsupervised PCA was carried out on NS and treated plants to demonstrate the system's suitability
331 (Fig. 2A). Indeed, the PCA score plot, built on the first and second principal components (PC1 and
332 PC2, respectively), revealed good discrimination of samples supplemented with all monochromatic
333 lights, highlighting model robustness, whilst the W supplemented plant area resulted overlapped to
334 NS plant area (Fig. 2A and Supplementary material, Table S2). The unsupervised PCA analysis, built
335 on the first two PCs that explained the 75.8 % of the total variability, highlighted, in the score plot, a
336 clear separation of groups (Fig. 2A). Looking at the loadings plot, the PC1 was mainly dominated by
337 n-acetyl-d-hexosamine, aspartic acid, glutamine, alanine, trehalose, 4-hydroxybutyric acid, glutamic
338 acid, fructose 6-phosphate, gallic acid, serine, epicatechin, glucose 6-phosphate, sulfuric acid,

339 whereas PC2 by γ-aminobutyric acid (GABA), phosphoric acid, epicatechin, lactulose, isoleucine,
340 glucose, alpha-lactose, galacturonic acid (Supplementary material, Table S2).

341 Similarly, the supervised PLS-DA analysis confirmed the separation of groups with the two
342 latent variables, explaining the 67.9 % of the total variance (Fig. 2B). The PLS-DA-derived VIP
343 scores (built on the first 25 metabolites with a VIP score > 1) revealed benzoic acid, 2-aminoethanol,
344 2-isopropylmalic acid, saccharic acid and aspartic acid as the ones with the highest VIP scores for the
345 five analyzed treatments (Fig. 4C and Supplementary material, Table S2).

346 As reported in the false scale colour of the VIP scores, the highest increase in metabolites was
347 observed in plants treated with B and G lights and, to a lesser extent, with R and W lights (Fig. 2C).
348 Concerning amino acids, known in the bibliography to be generally affected by monochromatic light
349 (Chen et al., 2014; Dhakal & Baek, 2014; Gao et al., 2022), the G and B light supplementation showed
350 the highest relative abundance of beta-alanine, glutamine, glutamic acid, GABA, allothreonine and
351 aspartic acid. On the contrary, during R supplementation only the glutamic acid was present in higher
352 content than control, whereas in plants exposed to W light, in comparison to NS, an accumulation of
353 serine, glutamine and GABA was observed (Fig. 2C).

354 A cluster analysis consisting of a heatmap, reporting in a false-color scale the variation of
355 metabolite concentration for each sample (only metabolites resulting from the ANOVA significantly
356 affected were used), confirmed, at a lower level, the total discrimination among all samples (Fig. 3),
357 whereas, at a higher level, B and G light supplemented plants, and, at the same time, also NS and W-
358 supplemented plants grouped together. Those results suggest similarity between G and B light
359 treatments and between W, R and NS light treatments. In fact, G and B light induced a general
360 accumulation of primary metabolites. On the contrary, in plants treated with R and W light, the level
361 of the metabolites was similar to NS (Fig. 3).

362 The pathway analysis further confirmed those observations, highlighting similar differences
363 in the pathways affected by the extra light supplementation. As reported in Table S3, W light
364 significantly affected only 2 pathways (linoleic and glycerophospholipid metabolism) when

compared to control. On the contrary, B and G lights affected 20 and 23 pathways, respectively, whereas R only 16 (Supplementary material, Table S2 and S3). In particular, R treatment was the only one affecting the TCA cyle and tyrosine metabolism in treated samples (Table S3).

3.3 UHPLC-HR-ESI-MS analysis results

The phytochemical profile of strawberry fruit from plants exposed to B, G, R, W LED supplementation and from NS plants was investigated. Results obtained from the analyses are reported in Table 1 for anthocyanin compounds and Table 2 for other phenolic classes. From a qualitative point of view, samples showed a very similar composition, characterized by the presence of six major classes of components: anthocyanins, flavonoids, ellagitannins, ellagic acid conjugates, cinnamic acid conjugates and proanthocyanidins. According to the literature, among anthocyanins, several pelargonidins and cyanidins were identified in their glycosylated forms, with pelargonidin hexoside as the most abundant molecule since two isomers of this compound were tentatively identified.

Moreover, the highest content of pelargonidin hexoside in the form of two isomers was found in strawberry fruit from plants supplemented with G, W and R light, whilst the lowest content in those from plants supplemented with B light. The latter monochromatic light also showed the lowest content of pelargonidin 3-O-(malonyl)glucoside and cyanidin 3-O-malonylglucoside if compared with the effect of the other lights under investigation. Instead, the R light showed the highest content of both anthocyanins. The annotated anthocyanins by MS data were previously isolated in *F.* × *ananassa* fruit, identified and quantified by external standards by different LC-MS techniques as reported in Table S4.

Among other phenolic classes, G light induced the increase of the majority of identified phenolic compounds when compared to the other treatments and to control plants (kaempferol O-malonyl-O-hexoside, kaempferol 3-coumaroylglucoside, pedunculagin, galloyl-diHHDP-glucose, digalloyl-tetraHHDP-diglucose, ellagic acid deoxyhexose, cinnamoyl glucose, procyanidin

pentamer, proanthocyanidin C1, procyanidin hexamer and procyanidin heptamer). Conversely to the anthocyanin accumulation, R light treatment promoted a lower abundance of other phenolic compounds (cinnamoyl xylosylglucose and cinnamoyl glucose) compared to NS, G and W treatments. However, quercetin 3-O-glucuronide increased in fruit from plants supplemented with R light when compared with the other treatments. The annotated phenolic compounds by MS data were previously isolated in *F.* × *ananassa* fruit, identified and quantified by external standards by different LC-MS techniques as reported in Table S4.

3.4. Fruit symptoms and disease development

Regardless of the light treatment, all *B. cinerea* inoculated fruit showed a typical development of grey mold symptoms/signs, which were not observed on uninoculated fruit. Until 24 hpi, no significant differences were observed among the AUDPC values of fruit collected from plants exposed to different light conditions. At 36 hpi, fruit collected from plants exposed to R light showed lower AUDPC values than those collected from plants exposed to NS or W, B and G lights. At 48 hpi, both fruit collected from plants exposed to R and B lights showed lower AUDPC values than those exposed to NS light. At 60 hpi, fruit collected from plants exposed to R light showed lower AUDPC values than those collected from plants exposed to W light. No significant differences were observed in terms of AUDPC at later analysis times (Table 3; Supplementary material, Fig. S2).

3.5. Gene expression analysis by qRT-PCR

Given the decrease of AUDPC in fruit from plants subjected to R light, the relative gene expression from non-inoculated (R) and *B. cinerea*-inoculated (R + Bc) fruit of plants grown under R light was compared with non-inoculated (NS) and inoculated (NS + Bc) control fruit of plants grown under non supplemented light. Results obtained at 48 hpi are reported in Fig. 4.

Among the analyzed genes, *beta-1,3-glucanase* (*F*×*aBG2-1)*, *Cellulose synthase-like protein D3* (*F*×*aCSLD3*), *Lignin forming anionic peroxidase* (*F*×*aLFAP*), *Polygalacturonase-inhibiting protein* (*F*×*aPGIP1*) and *Pectinesterase 41* (*F*×*aPE41*) increased their expression in inoculated fruit.

Conversely other genes like *Cynnamoil CoA reductase* (*F×aCCR1*), *Long-chain acyl-CoA synthetase 4* (*F×aLACS4*), *Disease resistant protein RPM1-like* (*F×aRPM1*), and *Pectate Lyase* (*F×aPECL*) did not show changes in their expression in inoculated fruit. The expression of *beta-1,3-glucanase* (*F×aBG2-1*), *polygalacturonase-inhibiting protein* (*F×aPGIP1*) and *pectinesterase 41* (*F×aPE41*) in inoculated fruit from R light treatment (R + Bc) resulted 3-fold higher than that found in inoculated control fruit (NS + Bc).

4. Discussion

Management of light in indoor cultivation is indisputable being crucial for plant growth and development. Supplemental light may also increase the yield and the nutritional/nutraceutical value of indoor productions through the "photomodulation" of targeted secondary metabolites (Rasiukevičiūtė et al., 2021). The main novelty of our experiments consists on the evaluation of supplemental LED light effects on strawberry fruit attributes, for which the literature is scarce when compared to experiments dealing with plants grown in fully-monochromatic environment. We offer the evidence that supplemental R light improves plant productivity and promotes specialized metabolite accumulation, in particular some well-represented anthocyanins in strawberry fruit. In addition, we propose molecular mechanisms by which R light supplementation delay the development of *B. cinerea* in postharvest.

The highest total fruit number and the average weight of single fruit observed in R light-supplemented plants in the present experiment is in agreement with previous findings (Gómez et al., 2013; Lu et al., 2012). Gómez et al. (2013) obtained a higher productivity in tomato plants using LED intracanopy lightning composed by 95 % R (peak wavelength at 627 nm) and 5 % B (peak at 450 nm) light (13.4 vs 9.1 kg plant^{-1} in R-enriched and controls, respectively). Lu et al. (2012) also observed that R light supplementation resulted in increased productivity in tomato plants (*Solanum lycopersicum* var. Momotaro Natsumi), supporting the positive role of R light on plant production as

observed in our experiment. Notably, a growth chamber experiment carried out with the strawberry variety Elsanta, the same used in the present work, showed a higher fruit number and a higher average fruit weight in plants exposed to B light than in those exposed to R light (Nadalini et al., 2017). This confirms that results from light enrichment experiments, as reported herein, might lead to dramatically different results from those obtained in plant grown in full "monochromatic" environments (Choi et al., 2015). In other cases, it has been demonstrated that the flux amplitude more than the LED color resulted in the highest increase of fruit number and overall yield (Choi et al., 2013). Besides the plant production, only slight significant differences were found in the color measurements among treatments in the present experiment. In particular, R-, G- and W-supplemented plants produced fruit with lower b^* (lower yellowness) when compared to NS and G-treated individuals. Supplemental R light also resulted in lower a^* (lower redness) while L^* values were not dissimilar to NS fruit, thereby suggesting only minor changes to overall colour perception of R-supplemented strawberry fruit. The impact of supplemental LED light was not significant in terms of fruit SSC and almost negligible in terms of fruit compactness and acidity, irrespectively to the LED colour. Conversely, in a previous enrichement experiment conducted in strawberry it was found the highest level of organic acids (citric and malic) in fruit from R-enriched plants as compared to B-supplemented and non-supplemented plants (Choi et al., 2015). It is conceivable that the different flux of supplemental LED light applied by Choi et al. (2015) and that provided in our experiment (i.e., 75 µmol m^{-2} s^{-1} *vs* 250 µmol m^{-2} s^{-1}, respectively) has to be considered as a possible factor responsible for such discrepancies.

In the GC–MS-driven untargeted metabolomics analysis, an overall accumulation of primary metabolites was found in fruit produced by plants supplemented with B and G light. As already reported by Dhakal and Baek (2014), amino acids metabolism is strongly affected in fruit subjected to B monochromatic light. However, some authors that analyzed mature tomatoes subjected to exclusive B light during the postharvest storage (Dhakal and Baek, 2014) found contrasting results. Indeed, specifying that the alanine synthesis occurs at the expense of glutamic acid and aspartic acid,

they observed an increase of alanine content in plants subjected to B light and a concomitantly decrease of the glutamic and aspartic acids (Dhakal and Baek, 2014). Similarly, both PLS-DA VIP scores and ANOVA analysis pointed out, under B light, an accumulation of alanine and reduced content of glutamic acid and aspartic acid, which content was higher than NS plants. A similar effect was also observed after G treatment, despite the level of alanine accumulated was lower than in plants under B light. However, the general decrease of primary metabolite contents (soluble sugars, amino acids and organic acids) in fruit exposed to R light observed in the present experiment was confirmed by Wu et al. (2020), analyzing the R light effect on postharvested pitaya fruit. Indeed, despite the different periods of exposure to light treatment, R light irradiation might accelerate the glycolysis and tricarboxylic acid (TCA) cycle at the enhanced resistance stage, leading to the decrease of soluble sugars and organic acids and slowing the TCA cycle at the senescence stage (Wu et al., 2020).

Unlike primary metabolites, fruit from plants under R light showed a higher content of two anthocyanins, particularly pelargonidin 3-O-(malonyl) glucoside and cyanidin 3-O-malonylglucoside, two anthocyanin classes with powerful antioxidant (Noda et al., 2002) and antitoxicant effects (Khandelwal and Abraham, 2014). The highest relative increase in fruit under R light was also seen for the quercetin 3-O-glucuronide, another specialized compounds with *a plethora* of health benefits for human health (Salehi et al., 2020). Though experiments carried out in postharvest fruit showed a negative correlation between anthocyanin and flavonoid accumulation and R light application, whilst a positive correlation was found between anthocyanin content and B light exposure (Li and Kubota, 2009; Xu et al., 2012), so far, only few studies (Choi et al., 2015; Zoratti et al., 2014) have investigated the relation between exposition of fruit to monochromatic light in pre-harvest and their polyphenolic content and profile. Zoratti et al. (2014), analyzing bilberry fruit (*Vaccinium myrtillus*) treated with monochromatic lights (R, B and Far-Red; FR), observed an increasing anthocyanin biosynthesis under monochromatic lights (R, B and FR) when compared with polychromatic and dark environments. They showed that monochromatic lights led to an up-regulation of the expression of *V. myrtillus anthocyanidin synthase* (*VmASN*) gene during the light

492 treatments irrespectively of the LED colour (Zoratti et al., 2014). A possible reason behind the highest
493 increase of anthocyanin and flavonoid concentration that we observed in fruit from plants
494 supplemented with R light might be the lack of a synergistic interaction between UV-B and the B
495 light (Arakawa et al., 1985) as usually occurs in field condition. In addition, as Choi et al. (2015) did
496 not observe any variation in strawberry fruit total anthocyanin and polyphenolic content with
497 supplementation of 75 µmol m^{-2} s^{-1} of R and B light, it can be assumed that the differences observed
498 in our experiment might be associated to the higher flux of supplemental monochromatic lights, i.e.,
499 250 µmol m^{-2} s^{-1}.

500 Other health-promoting secondary metabolites belonging to different phenolic classes such as
501 ellagic acid deoxyhesose and proanthocyanidin C1 resulted more abundant in fruit subjected to B and
502 G light treatment than in those subjected to R light and digalloyl-tetraHHPD-diglucose, procyanidin
503 pentamer, procyanidin hexamer and heptamer resulted more abundant in fruit subjected to B and G
504 light than those subjected to W light, confirming literature findings (Kobori et al., 2019). Kobori et
505 al. (2019) observed an increase of proanthocyanidins in raspberry fruit subjected to B light treatment
506 when compared with B:R light treatment at different concentrations. Indeed, they found an over-
507 expression of genes encoding key enzymes of the flavonoid pathway as chalcone synthase (CHS),
508 flavonoid 3′-hydroxylase (F3′H), flavonol synthase (FLS), dihydroflavonol 4-reductase (DFR) under
509 B light treatment (Kobori et al., 2019). Nevertheless, these results seem to be in contrast with the
510 lower anthocyanin content under B light since the biosynthetic pathway of anthocyanins and the other
511 flavonoids is the same except for the presence of anthocyanidin synthase enzyme. This enzyme
512 regulates anthocyanin biosynthesis, and, in this case, it might be responsible for lower anthocyanin
513 accumulation under B light. Our results were also confirmed by Kokalj et al. (2019) that achieved
514 higher catechin, epicatechin and procyanidins concentration in apple cultivars subjected to B light in
515 postharvest when compared with not irradiated apples. They found a higher phenylalanine ammonia
516 lyase (PAL) activity, another key enzyme of the phenolic pathway, under this monochromatic light.
517 This result can explain the higher content of some ellagitannins and ellagic acid conjugates found at

518 higher concentrations in fruit under B light, since PAL enzyme is the precursor enzyme of all phenolic
519 compounds and thus, also of gallic acid and, consequently, ellagic acid. More specifically, phenolic
520 synthesis control is done by transforming hydroxycinnamic acids, from the *trans* form (strong
521 inhibitors of PAL) to the *cis* form (less inhibitory) by B light (Lobiuc et al. 2017). At the same time,
522 UV receptors in plants, represented by cryptochromes and phototropins, are also B light sensors and
523 their involvement in the accumulation of phenolic acids under wavelengths close to UV ones may be
524 presumed (Lobiuc et al., 2017), also considering the little UV-B percentage in the greenhouse.
525 Interestingly, strawberries under G light showed the highest number of phenolic compounds
526 (11 compounds belonging to flavonoids, ellagitannins, ellagic acid conjugates and
527 proanthocyanidins) at higher concentrations when compared with the other treatments.
528 Green light can also drive the modulation of phenolic biosynthesis and accumulation (Landi
529 et al., 2020b). It commonly depresses the accumulation of flavonoids when compared to
530 polychromatic light (Landi et al., 2020b), and it can reverse the positive effects of monochromatic B
531 light in terms of flavonoid accumulation, contrasting our findings. However, few reports are available
532 in literature, which limits the accuracy of a general conclusion about the effect of G light on
533 polyphenol accumulation in strawberry fruit and the explanation of the positive correlation of
534 polyphenol concentration (e.g., digalloyl-tetraHHDP-glucose, ellagic acid deoxyhexose, procyanidin
535 pentamer, proanthocyanidin C1, procyanidin hexamer and heptamer) found between B and G light
536 treatments in the present work.
537 Indirect effect of color-selected narrow-band light, leading to modification of fruit
538 metabolism, can affect pathogen development. Previous studies confirmed our results that R light
539 was the most effective monochromatic light against the *B. cinerea* infection, followed by B light (Hui
540 et al., 2017; Khanama et al., 2005). For example, Khanama et al. (2005) observed the suppression of
541 lesion formation on broad bean leaves under R light treatment, resulting in the inhibition of *B. cinerea*
542 development. The authors offered the evidence that this pattern was related to a salicylic acid
543 signaling pathway and the enhancement of the catalase activity in broad bean leaves (Khanama et al.

2005). More specifically, Hui et al. (2017), analyzing the effect of R light on tomato leaves, observed that this monochromatic light can inhibit the development of grey mold due to a rapid defensive response by the plant. These finding were in agreement with Li et al. (2013), who observed a significantly improved activity of antioxidant enzymes (superoxide dismutase, catalase, peroxidases) in tomato leaves with a contemporary inhibition of the oxidative burst caused by the pathogen attack, resulting in a lower accumulation of O_2^- and H_2O_2 in plant tissues. For the sack of the truth, in other cases B light was found to be responsible for an enhanced suppression of *B. cinerea* symptom development in leaves/fruit (Imada et al., 2014; Kim et al., 2013). For example, Kim et al. (2013) observed lower symptoms of *B. cinerea* infection in B-treated plants, pointing out the possible involvement of proline accumulation and antioxidant process (as already shown for the R light treatment) as the reason behind the containment of fungus development.

Given the important R light effect on *B. cinerea* development, gene expression of the fundamental cell wall enzymes and proteins involved in defense response was analyzed in fruit collected from R supplemented plants in comparison with NS ones. Cell wall components (overall lignin, hemicellulose and pectins) are fundamental for the firmness of fruit and, consequently, for the *B. cinerea* penetration and invasion (Lee et al., 2021a). Cell wall biosynthesis' enzymes reinforce plant cells against fungus attack by deposition of lignin, strengthening cross-linkages, and changing wall component ratios (Hückelhoven, 2007). In the present work, genes *F×aBG2-1*, *F×aCSLD3*, *F×aLFAP*, *F×aPGIP1* and *F×aPE41* increased their expression in inoculated samples, confirming results reported in the literature (Lee et al., 2021a; Haile et al., 2019). In particular, genes *F×aBG2-1*, *F×aPGIP1* and *F×aPE41* showed higher expression in inoculated R treated fruit respect to inoculated NS ones, suggesting their expression is correlated with the decrease of disease observed in R treated fruit. The first one encodes a *beta-1,3-glucanase*, an enzyme that permits the degradation of *B. cinerea* beta-glucans; the second one encodes a *polygalacturonase-inhibiting protein* that recognizes and inhibits the fungus polygalacturonases, and the last one is related with a pectinesterase (*pectinesterase 41)* produced after the fungus attack, and that is also involved in cell wall thickening.

570 The induced production of these enzymes after wounding or in response to pathogen penetration has
571 been verified in different plant species including *F.* × *ananassa* (Lee et al., 2021a). However, to the
572 best of our knowledge, the upregulation of cell-wall genes under R light treatment was observed in
573 the present study for the first time. Their upregulation confirms the AUDPC results, supporting the
574 evidence of R light efficiency against *B. cinerea* proliferation in strawberry fruit.
575

576 ## 5. Conclusion

577 The present experiment demonstrated that a controlled light environment in pre-harvest may
578 improve the quality of strawberry fruit and defense mechanisms against pathogens in postharvest. In
579 particular, R light induced a higher yield and number of fruit than other monochromatic lights as well
580 as an increased accumulation of some anthocyanins and other flavonoids. Red light also resulted the
581 most effective monochromatic light against the *B. cinerea* infection likely through a stimulation of
582 targeted defensive secondary metabolites and promoting the upregulation of defensive genes after
583 fungal infection. Thus, the application of R light could play a twofold role in indoor strawberry
584 cultivation, i.e., enhancement of fruit quality from one side, and on the other side, reduction of
585 agrochemical inputs. Although in this study the effectiveness of R light has been shown to generally
586 improve (or retain) the quality of strawberry fruit, further analysis is necessary to evaluate the impact
587 of this treatment on the acceptability of fruit to consumers. This is especially crucial for postharvest
588 fruit quality and microbiological decontamination, whose objectives are to provide nutritious and safe
589 food acceptable to consumers.
590

591 **CRediT authorship contribution statement**

592 **Giulia Lauria**, **Ermes Lo Piccolo**, **Costanza Ceccanti**, **Fabrizio Araniti**, **Lorenzo Cotrozzi**,
593 **Michela Moriconi**, **Claudio Pugliesi, Rodolfo Bernardi**: Data curation; Formal analysis; Writing -

original draft; **Marco Landi**: Conseptualization; Project administration; Resources; Supervision; Validation; Visualization; Funding acquisition; **Lucia Guidi**, **Elisa Pellegrini**, **Tommaso Giordani**, **Cristina Nali**, **Luigi Sanità di Toppi**, **Luca Paoli**, **Fernando Malorgio**, **Paolo Vernieri**, **Rossano Massai**, **Damiano Remorini**, **Marco Landi**: Writing - review & editing.

Declaration of Competing Interest

The authors declare that they have no known competing financial interests or personal relationships that could have appeared to influence the work reported in this paper.

Acknowledgments

The manuscript is dedicated to the kind memory of Prof. Rodolfo Bernardi, who begun with us the experiment and never saw the end. The project was performed in the framework of the PRA 2020-2021 project "Fra*goal*" financed by the University of Pisa.

Appendix A. Supporting information

Supplementary data associated with this article can be found in the online version at…

References

Aaby, K., Mazur, S., Nes, A., Skrede, G., 2012. Phenolic compounds in strawberry (*Fragaria* x *ananassa* Duch.) fruit: Composition in 27 cultivars and changes during ripening. Food Chem. 132(1), 86–97. https://doi.org/10.1016/j.foodchem.2011.10.037

615 Al Murad, M., Razi, K., Jeong, B.R., Muthu Arjuna Samy, P., Muneer, S., 2021. Light emitting diodes
616 (Leds) as agricultural lighting: Impact and its potential on improving physiology, flowering,
617 and secondary metabolites of crops. Sustainability 13(4), 1985.
618 https://doi.org/10.3390/su13041985

619 Arakawa, O., Hori, Y., Ogata, R., 1985. Relative effectiveness and interaction of ultraviolet-B, red
620 and blue light in anthocyanin synthesis of apple fruit. Physiol. Plant. 64(3), 323–327.
621 https://doi.org/10.1111/j.1399-3054.1985.tb03347.x

622 Chen, C.C., Huang, M.Y., Lin, K.H., Wong, S.L., Huang, W.D., Yang, C.M., 2014. Effects of light
623 quality on the growth, development and metabolism of rice seedlings (*Oryza sativa* L.). Res. J.
624 Biotechnol. 9(4), 15–24.

625 Choi, H.G., Kwon, J.K., Moon, B.Y., Kang, N.J., Park, K.S., Cho, M.W., Kim, Y.C., 2013. Effect of
626 different light emitting diode (LED) lights on the growth characteristics and the phytochemical
627 production of strawberry fruit during cultivation. Hortic. Sci. Technol. 31(1), 56–64.
628 https://doi.org/10.7235/hort.2013.12100

629 Choi, H.G., Moon, B.Y., Kang, N.J., 2015. Effects of LED light on the production of strawberry
630 during cultivation in a plastic greenhouse and in a growth chamber. Sci. Hortic. 189, 22–31.
631 https://doi.org/10.1016/j.scienta.2015.03.022

632 Chong, J., Xia, J., 2020. Using metaboanalyst 4.0 for metabolomics data analysis, interpretation, and
633 integration with other omics data, in: Li, S. (Eds.), Computational methods and data analysis
634 for metabolomics. Humana Press, New York, pp. 337– 360.

635 Dhakal, R., Baek, K.H., 2014. Metabolic alternation in the accumulation of free amino acids and γ-
636 aminobutyric acid in post-harvest mature green tomatoes following irradiation with blue light.
637 Hortic. Environ. Biotechnol. 55(1), 36–41. https://doi.org/10.1007/s13580-014-0125-3

638 Edger, P.P., Poorten, T.J., VanBuren, R., Hardigan, M.A., Colle, M., McKain, M.R., Smith, R.D.,

639 Teresi, S.J., Nelson, A.D.L., Wai, C.M., Alger, E.I., Bird, K.A., Yocca, A.E., Pumplin, N., Ou,
640 S., Ben-Zvi, G., Brodt, A., Baruch, K., Swale, T., Shiue, L., Acharya, C.B., Cole, G.S., Mower,
641 J.P., Childs, K.L., Jiang, N., Lyons, E., Knapp, S.J., 2019. Origin and evolution of the octoploid
642 strawberry genome. Nat. Gen. 51, 541–547. https://doi.org/10.1038/s41588-019-0356-4

643 Fausto, C., Araniti, F., Mininni, A.N., Crecchio, C., Scagliola, M., Bleve, G., Dichio, B., Sofo, A.,
644 2021. Differential olive grove management regulates the levels of primary metabolites in xylem
645 sap. Plant Soil 460, 281–296. https://doi.org/10.1007/s11104-020-04800-0

646 Gallé, Á., Czékus, Z., Tóth, L., Galgóczy, L., Poór, P., 2021. Pest and disease management by red
647 light. Plant Cell Environ. 44(10), 3197–3210. https://doi.org/10.1111/pce.14142

648 Gao, S., Kong, Y., Lv, Y., Cao, B., Chen, Z., Xu, K., 2022. Effect of different LED light quality
649 combination on the content of vitamin C, soluble sugar, organic acids, amino acids, antioxidant
650 capacity and mineral elements in green onion (*Allium fistulosum* L.). Food Res. Int. 156,
651 111329. https://doi.org/10.1016/j.foodres.2022.111329

652 Gómez, C., Morrow, R.C., Bourget, C.M., Massa, G.D., Mitchell, C.A., 2013. Comparison of
653 Intracanopy Light-emitting Diode Towers and Overhead High-pressure Sodium Lamps for
654 Supplemental Lighting of Greenhouse-grown Tomatoes. HortTechnology 23(1), 93–98.
655 https://doi.org/10.21273/HORTTECH,23,1,93

656 Haile, Z.M., Nagpala-De Guzman, E.G., Moretto, M., Sonego, P., Engelen, K., Zoli, L., Moser, C.,
657 Baraldi, E., 2019. Transcriptome profiles of strawberry (*Fragaria vesca*) fruit interacting with
658 *Botrytis cinerea* at different ripening stages. Front. Plant Sci. 10, 1131.
659 https://doi.org/10.3389/fpls.2019.01131

660 Horai, H., Arita, M., Kanaya, S., Nihei, Y., Ikeda, T., Suwa, K., Ojima, Y., Tanaka, K., Tanaka, S.,
661 Aoshima, K., Oda, Y., Kakazu, Y., Kusano, M., Tohge, T., Matsuda, F., Sawada, Y., Hirai, M.
662 Y., Nakanishi, H., Ikeda, K., Akimoto, N., Maoka, T., Takahashi, H., Ara, T., Sakurai, N.,

Suzuki, H., Shibata, D., Neumann, S., Iida, T., Tanaka, K., Funatsu, K., Matsuura, F., Soga, T., Taguchi, R., Saito, K, Nishioka, T., 2010. MassBank: a public repository for sharing mass spectral data for life sciences. J. Mass Spectrom. 45, 703–714. https://doi.org/10.1002/jms.1777

Huang, J.Y., Xu, F., Zhou, W., 2018. Effect of LED irradiation on the ripening and nutritional quality of post-harvest banana fruit. J. Sci. Food Agric. 98(14), 5486–5493. https://doi.org/10.1002/jsfa.9093

Hückelhoven, R. (2007). Cell wall–associated mechanisms of disease resistance and susceptibility. Annu. Rev. Phytopathol. 45, 101–127. https://doi.org/10.1146/annurev.phyto.45.062806.094325

Hui, X.U., Fu, Y.N., Li, T.L., Rui, W.A.N.G., 2017. Effects of different LED light wavelengths on the resistance of tomato against *Botrytis cinerea* and the corresponding physiological mechanisms. J. Integr. Agric. 16(1), 106–114. https://doi.org/10.1016/S2095-3119(16)61435-1

Imada, K., Tanaka, S., Ibaraki, Y., Yoshimura, K., Ito, S., 2014. Antifungal effect of 405-nm light on *Botrytis cinerea*. Lett. Appl. Microbiol. 59(6), 670–676. https://doiotg/10.1111/lam.12330

Khandelwal, N., Abraham, S.K., 2014. Intake of anthocyanidins pelargonidin and cyanidin reduces genotoxic stress in mice induced by diepoxybutane, urethane and endogenous nitrosation. Environ. Toxicol. Pharmacol. 37(2), 837–843. https://doi.org/10.1016/j.etap.2014.02.012

Khanama, N.N., Uenoa, M., Kiharab, J., Hondac, Y., Arase, S., 2005. Suppression of red light-induced resistance in broad beans to *Botrytis cinerea* by salicylic acid. Physiol. Mol. Plant Pathol. 6, 20–29. https://doi.org/10.1016/j.pmpp.2005.03.006

Kim, K., Kook, H.S., Jang, Y.J., Lee, W.H., Seralathan, K.K., Chae, J.C., Lee, K.J., 2013. The effect of blue-light-emitting diodes on antioxidant properties and resistance to *Botrytis cinerea* in tomato. J. Plant Pathol. Microbiol. 4, 203–208. https://doi.org/10.4172/2157-7471.1000203

687 Kim, B.S., Lee, H.O., Kim, J.Y., Kwon, K.H., Cha, H.S., Kim, J.H., 2011. An effect of light emitting
688 diode (LED) irradiation treatment on the amplification of functional components of immature
689 strawberry. Hortic. Environ. Biotechnol. 52(1), 35–39. https://doi,org/10,1007/s13580-011-
690 0189-2

691 Kobori, R., Hashimoto, S., Koshimizu, H., Yakami, S., Hirai, M., Noro, K., Kawasaki, T; Saito, A.,
692 2019. Flavan-3-ols content in red raspberry leaves increases under blue LED-light irradiation.
693 Metabolites 9(3), 56. https://doi.org/10.3390/metabo9030056

694 Kokalj, D., Zlatić, E., Cigić, B., Kobav, M. B., Vidrih, R., 2019. Post-harvest flavonol and
695 anthocyanin accumulation in three apple cultivars in response to blue-light-emitting diode light.
696 Sci. Hortic. 257, 108711. https://doi.org/10.1016/j.scienta.2019.108711

697 Landi, M., Araniti, F., Flamini, G., Lo Piccolo, E., Trivellini, A., Abenavoli, M.R., Guidi, L.,2020a.
698 "Help is in the air": volatiles from salt-stressed plants increase the reproductive success of
699 receivers under salinity. Planta 251, e48. https://doi.org/10.1007/s00425-020-03344-y

700 Landi, M., Zivcak, M., Sytar, O., Brestic, M., Allakhverdiev, S.I., 2020b. Plasticity of photosynthetic
701 processes and the accumulation of secondary metabolites in plants in response to
702 monochromatic light environments: A review. Biochim. Biophys. Acta Bioenerg. 1861(2),
703 148131. https://doi.org/10.1016/j.bbabio.2019.148131

704 Lauria, G., Lo Piccolo, E., Pellegrini, E., Bellini, E., Giordani, T., Guidi, L., Lorenzini, G., Malorgio,
705 F., Massai, R., Nali, C., Paoli, L., Remorini, D., Sanità di Toppi, L., Vernieri, P., Landi, M.,
706 2021. Photosynthetic traits and biochemical responses in strawberry (*Fragaria* x *ananassa*
707 Duch,) leaves supplemented with LED lights. Photosynthetica 59(4), 557–569.
708 https://doi.org/10.32615/ps.2021.048

709 Lee, K., Lee, J.G., Min, K., Choi, J.H., Lim, S., Lee, E.J., 2021a. Transcriptome analysis of the fruit
710 of two strawberry cultivars "Sunnyberry" and "Kingsberry" that show different susceptibility
711 to *Botrytis cinerea* after harvest. Int. J. Mol. Sci. 22(4), 1518.

https://doi.org/10.3390/ijms22041518

Lee, H.-E., Manivannan, A., Lee, S.Y., Han, K., Yeum, J.-G., Jo, J., Kim, J., Rho, I.R., Lee, Y.-R., Lee, E.S., Kang, B.-C., Kim, D.-S., 2021b. Chromosome level assembly of homozygous inbred line 'Wongyo 3115' facilitates the construction of a high-density linkage map and identification of QTLs associated with fruit firmness in octoploid strawberry (*Fragaria* × *ananassa*). Front. Plant Sci. 12, 696229. https://doi.org/10.3389/fpls.2021.696229

Li, X., Yue, H., Wang, S., Huang, L.Q., Ma, J., Guo, L.P., 2013. Research of different effects on activity of plant antioxidant enzymes. Chin. Med. J. 38, 973–978. https://doi.org/10.4268/cjcmm20130709

Li, Q., Kubota, C., 2009. Effects of supplemental light quality on growth and phytochemicals of baby leaf lettuce. Environ. Exp. Bot. 67(1), 59–64. https://doi.org/10.1016/j.envexpbot.2009.06.011

Lin, R.L., Chang, Y.C., Lee, C.C., 2013. Optimal design of LED array for single-loop CCM buck–boost LED driver. IEEE Trans. Ind. Appl. 49(2), 761–768. https://doi.org/10.1109/IAS.2011.6074373

Lobiuc, A., Vasilache, V., Pintilie, O., Stoleru, T., Burducea, M., Oroian, M., Zamfirache, M. M., 2017. Blue and red LED illumination improves growth and bioactive compounds contents in acyanic and cyanic *Ocimum basilicum* L. microgreens. Molecules 22(12), 2111 https://doi.org/10.3390/molecules22122111

Lu N., Maruo T., Johkan M., Hohjo M., Tsukagoshi S., Ito Y., Ichmura T. Shinohara Y., 2012. Effects of supplemental lighting with light-emitting diodes (LEDs) on tomato yield and quality of single-truss tomato plants grown at high planting density. Environ. Control. Biol. 50(1), 63–74. https://doi.org/10.2525/ecb.50.63

734 Nadalini, S., Zucchi, P., Andreotti, C., 2017. Effects of blue and red led lights on soilless cultivated
735 strawberry growth performances and fruit quality. Eur. J. Hortic. Sci. 82, 1 12–20.
736 https://doi,org/10,17660/eJHS,2017/82,1,2

737 Natali, L.,Vangelisti, A., Guidi, L., Remorini, D., Cotrozzi, L., Lorenzini, G., Nali, C., Pellegrini, E.,
738 Trivellini, A., Vernieri, P., Landi, M., Cavallini, A., Giordani, T., 2018. How *Quercus ilex* L.
739 saplings face combined salt and ozone stress: a transcriptome analysis. BMC Genom. 19, 872.
740 https://doi.org/10.1186/s12864-018-5260-2

741 Ngcobo, B.L., Bertling, I., Clulow, A.D., 2020. Preharvest illumination of cherry tomato reduces
742 ripening period, enhances fruit carotenoid concentration and overall fruit quality. J. Hortic. Sci.
743 Biotechnol. 95(5), 617–627. https://doi.org/10.1080/14620316.2020.1743771

744 Noda, Y., Kaneyuki, T., Mori, A., Packer, L. (2002). Antioxidant activities of pomegranate fruit
745 extract and its anthocyanidins: delphinidin, cyanidin, and pelargonidin. J. Agric. Food Chem.
746 50(1), 166–171. https://doi.org/10.1021/jf0108765

747 Petrasch, S., Knapp, S.J., Van Kan, J.A., Blanco-Ulate, B., 2019. Grey mould of strawberry, a
748 devastating disease caused by the ubiquitous necrotrophic fungal pathogen *Botrytis cinerea*.
749 Mol. Plant Pathol. 20(6), 877–892. https://doi.org/10.1111/mpp.12794

750 Rasiukevičiūtė, N., Brazaitytė, A., Vaštakaitė-Kairienė, V., Kupčinskienė, A., Duchovskis, P.,
751 Samuolienė, G., Valiuškaitė, A., 2021. The Effect of Monochromatic LED Light Wavelengths
752 and Photoperiods on *Botrytis cinerea*. J. Fungi 7(11), 970. https://doi.org/10.3390/jof7110970

753 Salehi, B., Machin, L., Monzote, L., Sharifi-Rad, J., Ezzat, S.M., Salem, M.A., Merghany, R.M., El
754 Mahdy, N.M., Kılıç, C.S., Sytar, O:, Sharifi-Rad, M., Sharopov, F., Martins, N., Martorell, M.,
755 Cho, W.C., 2020. Therapeutic potential of quercetin: new insights and perspectives for human
756 health. Acs Omega 5(20), 11849–11872. https://doi.org/10.1021/acsomega.0c01818

Sansone, S.A., Fan, T., Goodacre, R., Griffin, J.L., Hardy, N.W., Kaddurah-Daouk, R., Kristal, B.S., Lindon, J., Mendes, P., Morrison, N., Nikolau, B., Robertson, D., Summer, L.W., Tayor, C., van der Werf, M., van Ommen, B., Fiehn, O., 2007. The metabolomics standards initiative. Nat. Biotechnol. 25, 846–849. https://doi.org/10.1038/nbt0807-846b

Simko, I., Piepho, H.P., 2012 The area under the disease progress stairs: Calculation, advantage, and application. Phytopathology 102, 381–389. https://doi.org/10.1094/PHYTO-07-11-0216

Xu, H.L., Xu, Q., Li, F., Feng, Y., Qin, F. Fang, W., 2012. Applications of xerophytophysiology in plant production-LED blue light as a stimulus improved the tomato crop. Sci. Hortic. 148, 190–196. https://doi.org/10.1016/j.scienta.2012.06.044

Wu, Q., Gao, H., Zhang, Z., Li, T., Qu, H., Jiang, Y., Yun, Z., 2020. Deciphering the metabolic pathways of pitaya peel after post-harvest red light irradiation. Metabolites 10(3), 108. https://doi.org/10.3390/metabo10030108

Zoratti, L., Sarala, M., Carvalho, E., Karppinen, K., Martens, S., Giongo, L., Häggman, H., Jaakola, L., 2014. Monochromatic light increases anthocyanin content during fruit development in bilberry. BMC Plant Biol. 14(1), 110. https://doi.org/10.1186/s12870-014-0377-1

Tables

Table 1. Retention time (t_R) and mass spectral data of the identified anthocyanins in strawberry fruit from plants exposed to blue (B), green (G), red (R), polychromatic (W) and no (NS, i.e., controls) LEDs supplementation. Each value is the mean ± standard deviation of three replicates. Means keyed with the same letter in bold are not significantly different for $p \leq 0.05$ following one-way ANOVA using Fisher's *post-hoc* least significant difference test with different light treatment as a source of variability.

t_R	$[M]^+$	MS^2	Error ppm	Formula	Compound	Peak Area * 10^6				
						B	**G**	**W**	**R**	**NS**
1.48	579.1496	271.06	-0.173	$C_{30}H_{27}O_{12}$	Pelargonidin 3-O-(6-p-coumaroyl)-hexoside	72.3±5.9a	73.8±32.5a	84.1±11.3a	97.8±19.2a	55.7±10.4a
1.66	433.1128	271.06	+0.209	$C_{21}H_{21}O_{10}$	Pelargonidin hexoside (2 isomers)	1550.8±16.9c	3368.7±647.8a	3753.0±670.4a	3137.8±488.6ab	2305.9±265.3b
1.94	563.1135	287.05	-0.550	$C_{30}H_{27}O_{11}$	Cyanidin derivative	23.4±0.5a	19.9±8.7a	21.1±2.7a	17.0±2.3a	16.5±2.6a
2.24	519.1133	271.06	+0.520	$C_{24}H_{23}O_{13}$	Pelargonidin 3-O-(malonyl)glucoside	194.2±12.2c	790.6±164.0ab	714.8±62.9b	976.1±221.7a	560.6±17.4b
2.94	533.1292	271.06	+0.450	$C_{25}H_{25}O_{13}$	Pelargonidin derivative	339.6±84.4a	405.7±172.7a	378.5±108.7a	277.9±85.9a	329.6±25.3a
3.31	449.1077	287.05	-0.445	$C_{21}H_{21}O_{11}$	Cyanidin 3-O-glucoside	13.9±0.1a	26.2±17.2a	32.3±8.5a	28.1±6.2a	23.0±1.6a
3.63	535.1083	287.05	+0.206	$C_{24}H_{23}O_{14}$	Cyanidin 3-O-malonylglucoside	9.0±0.9c	67.3±7.5ab	83.8±31.6ab	92.0±25.2a	52.1±9.7b
4.02	477.1026	287.05	-0.314	$C_{22}H_{21}O_{12}$	Cyanidin derivative	11.0±3.6a	18.3±13.6a	15.1±5.5a	10.3±3.9a	12.7±3.7a

4.32	549.1241	287.05	+0.492	$C_{25}H_{25}O_{14}$	Cyanidin derivative	57.3±18.2a	25.9±13.2a	57.0±14.0a	39.6±11.1a	47.5±10.4a
4.81	595.1444	287.05	-0.353	$C_{30}H_{27}O_{13}$	Cyanidin-3- (coumaroyl)- hexoside	0.8±0.2a	10.7±9.4a	7.2±3.4a	5.3±1.3a	7.4±4.4a

Table 2. Retention time (t_R) and mass spectral data of the identified polyphenols in strawberry fruit from plants exposed to blue (B), green (G), red (R), polychromatic (W) and no (NS, i.e., controls) LEDs supplementation. Each value is the mean ± standard deviation of three replicates. Means keyed with the same letter in bold are not significantly different for $p \leq 0.05$ following one-way ANOVA using Fisher's *post-hoc* least significant difference test with different light treatment as a source of variability.

t_R	[M-H]$^-$	MS^2	Error ppm	Formula	Compound	Peak Area * 10^6				
						B	**G**	**W**	**R**	**NS**
Flavonoids										
8.00	477.0686	301.04	+2.452	$C_{21}H_{18}O_{13}$	Quercetin 3-O-glucuronide	67.8±1.3b	38.1±3.7c	31.4±10.5c	110.0±23.2a	37.0±0.6c
8.61	447.0934	285.04	+0.291	$C_{21}H_{20}O_{11}$	Kaempferol glucoside	57.4±1.2a	76.1±14.7a	62.4±11.6a	59.2±7.3a	77.4±10.2a
8.82	461.0729	285.04	+0.716	$C_{21}H_{18}O_{12}$	Kaempferol 3-O-glucuronide	61.3±11.5a	44.5±3.1a	43.4±15.2a	49.6±7.9a	52.8±10.4a
9.44	533.0940	285.04	+0.131	$C_{24}H_{22}O_{14}$	Kaempferol O-malonyl-O-hexoside	121.8±10.1b	166.8±32.6a	129.9±21.1b	127.2±7.6b	182.7±8.6a
11.47	593.1304	285.04	+0.624	$C_{30}H_{26}O_{13}$	Kaempferol 3-coumaroylglucoside	69.8±11.0b	132.7±22.4a	66.1±6.4b	85.4±25.2b	63.8±11.6b
Ellagitannins										
3.43	783.0697		+1.341	$C_{34}H_{24}O_{22}$	Pedunculagin	12.9±1.5ab	13.4±2.6a	7.8±1.0b	9.4±0.4b	11.4±1.9ab
4.49	633.0740	301.00	+0.995	$C_{27}H_{22}O_{18}$	Strictinin	13.3±3.1a	15.2±4.0a	10.2±0.2a	10.6±1.3a	14.1±2.6a
7.21	466.0264 ([M-H]$^{2-}$)	772.86, 679.43, 301.00	+0.150	$C_{41}H_{26}O_{26}$	Castalgin	25.3±5.3a	34.3±9.0a	27.8±2.4a	22.0±2.2a	24.2±4.6a

8.13	467.0361 ([M-H]$^{2-}$)	888.29, 301.00	-0.128	$C_{41}H_{28}O_{26}$	Galloyl-diHHDP-glucose (casuarictin)	50.4±12.0ab	69.9±16.7a	40.9±5.2b	43.9±3.6b	62.2±7.4a
11.01	934.0728 ([M-H]$^{2-}$)	1567.14, 935.07, 301.00	+1.103	$C_{82}H_{54}O_{52}$	Digalloyl-tetraHHDP-diglucose/ Sanguin H-6 isomer	155.9±15.4a	199.7±31.8a	85.9±11.4b	119.0±16.7ab	134.8±58.6ab
Ellagic acid conjugates										
7.53	447.0571	301.00	+1.051	$C_{20}H_{16}O_{12}$	Ellagic acid deoxyhexose	81.5±8.8a	90.0±16.1a	58.3±1.1ab	52.1±18.3b	80.3±15.0a
7.63	300.9990		+0.100	$C_{14}H_6O_8$	Ellagic acid	118.8±25.4a	132.6±36.4a	84.0±5.0a	85.2±18.6a	118.6±12.8a
Cinnamic acid conjugates										
3.92	325.0929	145.03, 163.04, 187.04	-0.185	$C_{15}H_{18}O_8$	*p*-Coumaric acid 4-O-glucoside (isomer I)	748.1±97.3a	948.8±290.9a	1041.3±163.9a	926.3±293.6a	1091.8±173.7a
4.14	325.0932	145.03, 163.04, 187.04	+0.861	$C_{15}H_{18}O_8$	*p*-Coumaric acid 4-O-glucoside (isomer II)	148.0±27.6a	175.7±18.9a	196.4±27.0a	159.5±33.8a	169.3±27.4a
6.68	487.1456 ([M+HCOO]$^-$)	441.14, 147.04	-0.164	$C_{20}H_{27}O_{11}$	Cinnamoyl xylosylglucose	73.7±15.9bc	110.5±23.6ab	170.0±19.0a	53.6±7.6c	135.3±61.9a
6.87	355.1034 ([M+HCOO]$^-$)	309.10, 147.04	-0.282	$C_{15}H_{19}O_7$	Cinnamoyl glucose	577.2±142.9ab	641.3±37.3a	739.9±34.5a	261.3±26.0c	607.4±31.9ab
Proanthocyanidins										
3.55	577.1354	451.10, 425.09, 289.07	+0.502	$C_{30}H_{26}O_{12}$	Procyanidin dimer	278.0±31.2a	329.3±68.0a	250.3±15.1a	264.5±30.1a	241.6±18.1a
3.77	289.0718	245.08, 109.03	+0.173	$C_{15}H_{14}O_6$	Catechin	1013.5±141.1a	1114.3±220.3a	945.0±65.8a	913.7±75.1a	805.4±51.3a

4.41	865.1998	695.14, 407.08, 289.07, 287.06	+1.422	$C_{45}H_{38}O_{18}$	Procyanidin trimer	135.1±28.2a	149.3±31.0a	116.6±7.8a	135.5±14.5a	105.6±6.4a
4.71	561.1408	435.11, 289.07, 271.06	+1.034	$C_{30}H_{26}O_{11}$	Propelargonidin dimer	49.0±9.2a	55.4±16.1a	45.4±6.0a	42.6±3.7a	43.0±0.7a
5.72	576.1276 ([M-H]$^{2-}$)	575.12, 451.10, 289.07	+1.725	$C_{60}H_{50}O_{24}$	Procyanidin tetramer	194.0±38.3a	259.6±57.4a	185.8±8.0a	187.1±24.4a	176.5±15.6a
6.08	720.1601 ([M-H]$^{2-}$)	289.07	+1.500	$C_{75}H_{62}O_{30}$	Procyanidin pentamer	241.2±23.9a	222.1±77.4a	161.3±26.1b	185.5±29.9ab	174.8±13.9ab
6.73	865.1995	407.07, 289.07, 287.06	+1.133	$C_{45}H_{38}O_{18}$	Proanthocyanidin C1 (catechin trimer)	55.0±5.9a	65.0±14.2a	43.9±1.9ab	37.2±4.3b	47.0±2.8ab
7.92	864.1915 ([M-H]$^{2-}$)	1463.81, 289.07, 287.06	+0.949	$C_{90}H_{74}O_{36}$	Procyanidin hexamer	119.8±7.4a	119.4±25.7a	85.5±6.6ab	110.0±17.4a	88.9±7.0ab
9.60	1008.7253 ([M-H]$^{2-}$)	407.07, 289.07, 287.06	+0.525	$C_{105}H_{86}O_{42}$	Procyanidin heptamer	76.6±7.1a	84.3±17.4a	55.3±6.0b	73.3±5.9ab	58.5±5.0b

Table 3. Data from Area Under the Disease Progress Curve (AUDPC) of *Botrytis cinerea*-inoculated fruit collected from plants exposed to blue (B), green (G), red (R), polychromatic (W) and no (NS, i.e., controls) LEDs supplementation. Each value is the mean ± standard deviation of 7-22 replicates. Means keyed with the same letter are not significantly different for $p \leq 0.05$ following one-way ANOVA using the Tukey's HSD *post-hoc* test with different light treatments as a source of variation.

Treatment	**Hours post inoculation**								
	0	12	24	36	48	60	72	84	96
B	<0.1 ± <0.1a	13.9 ± 2.9a	32.2 ± 7.0a	50.8 ± 9.3bc	78.3 ± 12.0b	105.0 ± 12.4ab	139.3 ± 16.2a	186.3 ± 19.3a	245.3 ± 23.4a
G	<0.1 ± 0.1a	13.1 ± 2.4a	30.8 ± 5.1a	53.2 ± 5.5bc	82.4 ± 8.9ab	108.0 ± 13.4ab	141.0 ± 17.5a	182.1 ± 20.8a	232.9 ± 24.7a
W	<0.1 ± 0.4a	13.6 ± 2.7a	32.1 ± 6.6a	58.8 ± 6.1ab	86.0 ± 8.7ab	110.4 ± 7.6a	147.3 ± 12.0a	191.3 ± 16.2a	248.0 ± 21.6a
R	<0.1 ± 0.3a	13.3 ± 2.5a	30.4 ± 6.7a	46.9 ± 8.4c	73.9 ± 14.3b	92.0 ± 13.5b	132.6 ± 19.1a	181.6 ± 23.8a	242.6 ± 27.7a
NS	<0.1 ± 0.2a	14.3 ± 3.0a	35.8 ± 8.1a	64.0 ± 13.0a	95.0 ± 20.1a	107.0 ± 8.5ab	137.1 ± 13.8a	177.6 ± 19.1a	229.3 ± 22.8a

Captions of Figures

Fig. 1. Number (A), weight (B), lightness (C), redness (D), yellowness (E), firmness (F), solid soluble content (SSC; G) and titratable acidity (TA; H) of fruit collected from plants exposed to blue (B), green (G), polychromatic (W), red (R) and no (NS, i.e., controls) LEDs supplementation. Each value is the mean ± standard deviation of 10 replicates. Means keyed with the same letter are not significantly different for $p \leq 0.05$ following one-way ANOVA using the Tukey's HSD *post-hoc* test with different light treatments as a source of variation.

Fig. 2. Discrimination through principal component analysis (PCA) and partial least square discriminant analysis (PLS-DA) of fruit from plants exposed to blue (B), green (G), red (R), polychromatic (W) and no (NS, i.e., controls) LEDs supplementation analyzed basing on metabolomics analysis. (*A*) PCA and (*B*) PLS-DA showing score plots treatments by virtue of the first two principal components (PCs). (*C*) Variable importance of projection (VIP) features for the treatments from PLS-DA analysis.

Fig. 3. Overlay heatmap of the top 75 metabolites profiles, resulting from the ANOVA analysis (LSD test with $p \leq 0.05$ and FDR ≤ 0.05), differentially produced in fruit from plants exposed to blue (B), green (G), red (R), polychromatic (W) and no (NS, i.e., controls) LEDs supplementation. Each rectangle represents the different light treatment's effect on every metabolite's relative abundance using a false-color scale. Dark red and green colors indicate the increase and decrease of relative metabolite abundances, respectively.

Fig. 4. Relative expression levels of genes encoding enzymes related to *B. cinerea* challenge to *Fragaria* × *ananassa* fruit. The relative gene expression from non-inoculated (R) and *B. cinerea*-inoculated (R + Bc) fruit of plants grown under R light was compared with non-inoculated (NS) and inoculated (NS + Bc) control fruit of plants grown under non-supplemented light. The transcript levels were detected after 48 hpi. Each value is the mean ± standard deviation. Different letters indicate

statistically significant differences after two-way ANOVA according to *post-hoc* Tukey's HSD test ($p \leq 0.05$). Gene list is available in Supplementary material, Table S1.

Figures

Fig. 1

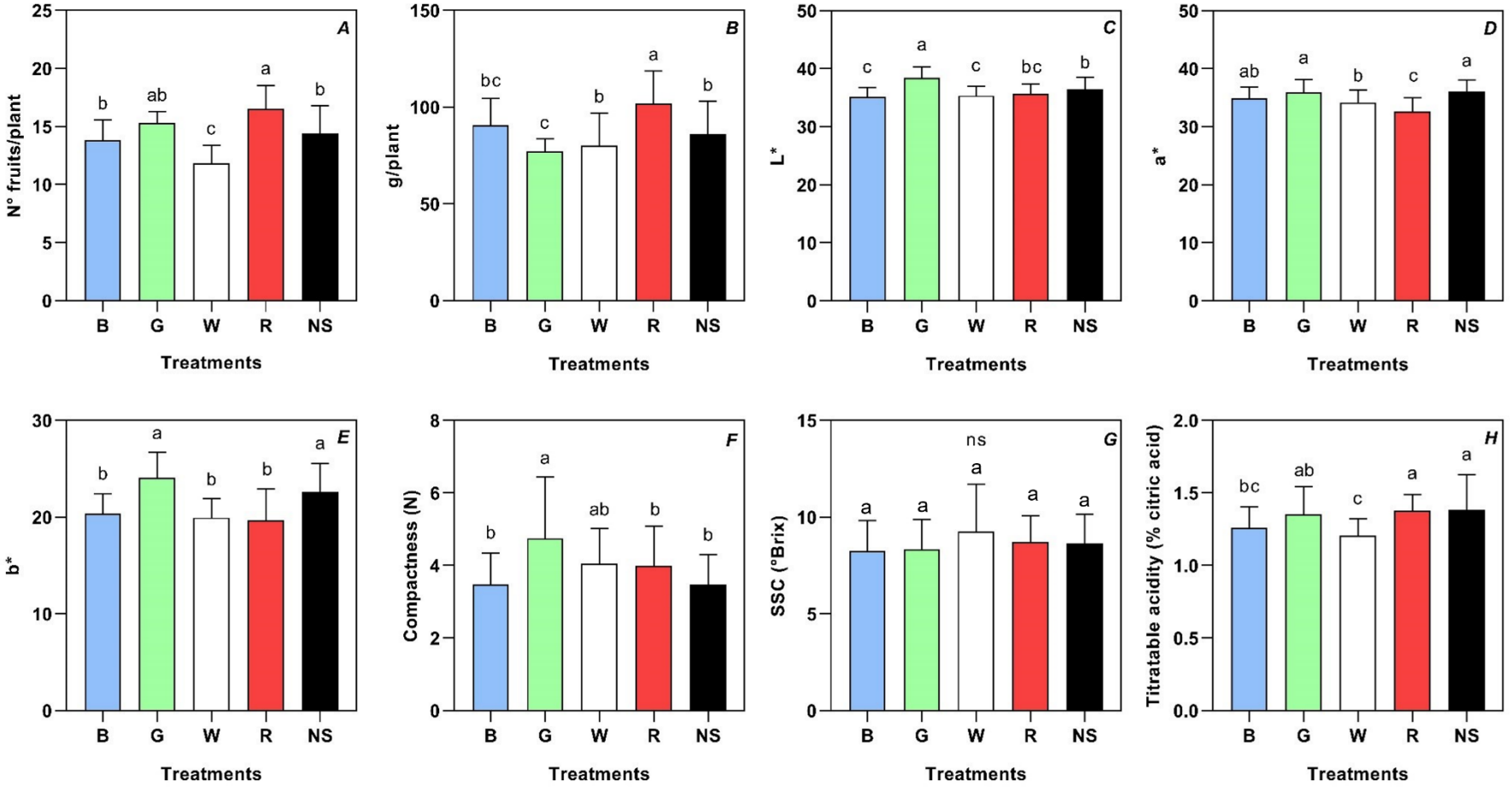

Fig. 2

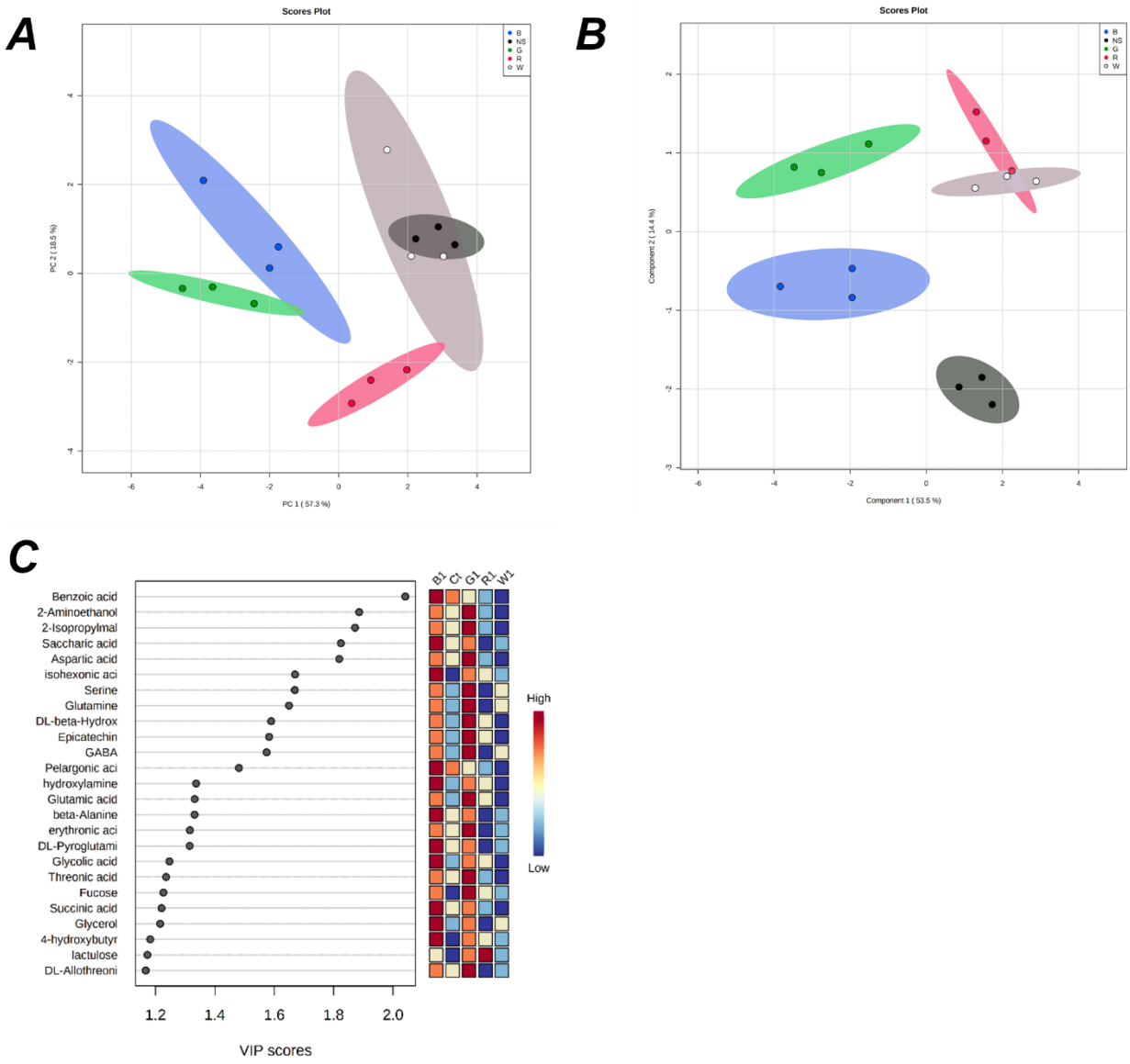
A
Scores Plot
B
NS
G
R
W
PC 1 (57.3 %)
PC 2 (18.5 %)
B
Scores Plot
Component 1 (53.5 %)
Component 2 (14.4 %)
C
Benzoic acid
2-Aminoethanol
2-Isopropylmal
Saccharic acid
Aspartic acid
isohexonic aci
Serine
Glutamine
DL-beta-Hydrox
Epicatechin
GABA
Pelargonic aci
hydroxylamine
Glutamic acid
beta-Alanine
erythronic aci
DL-Pyroglutami
Glycolic acid
Threonic acid
Fucose
Succinic acid
Glycerol
4-hydroxybutyr
lactulose
DL-Allothreoni
B1
C1
G1
R1
W1
High
Low
1.2
1.4
1.6
1.8
2.0
VIP scores

Fig. 3

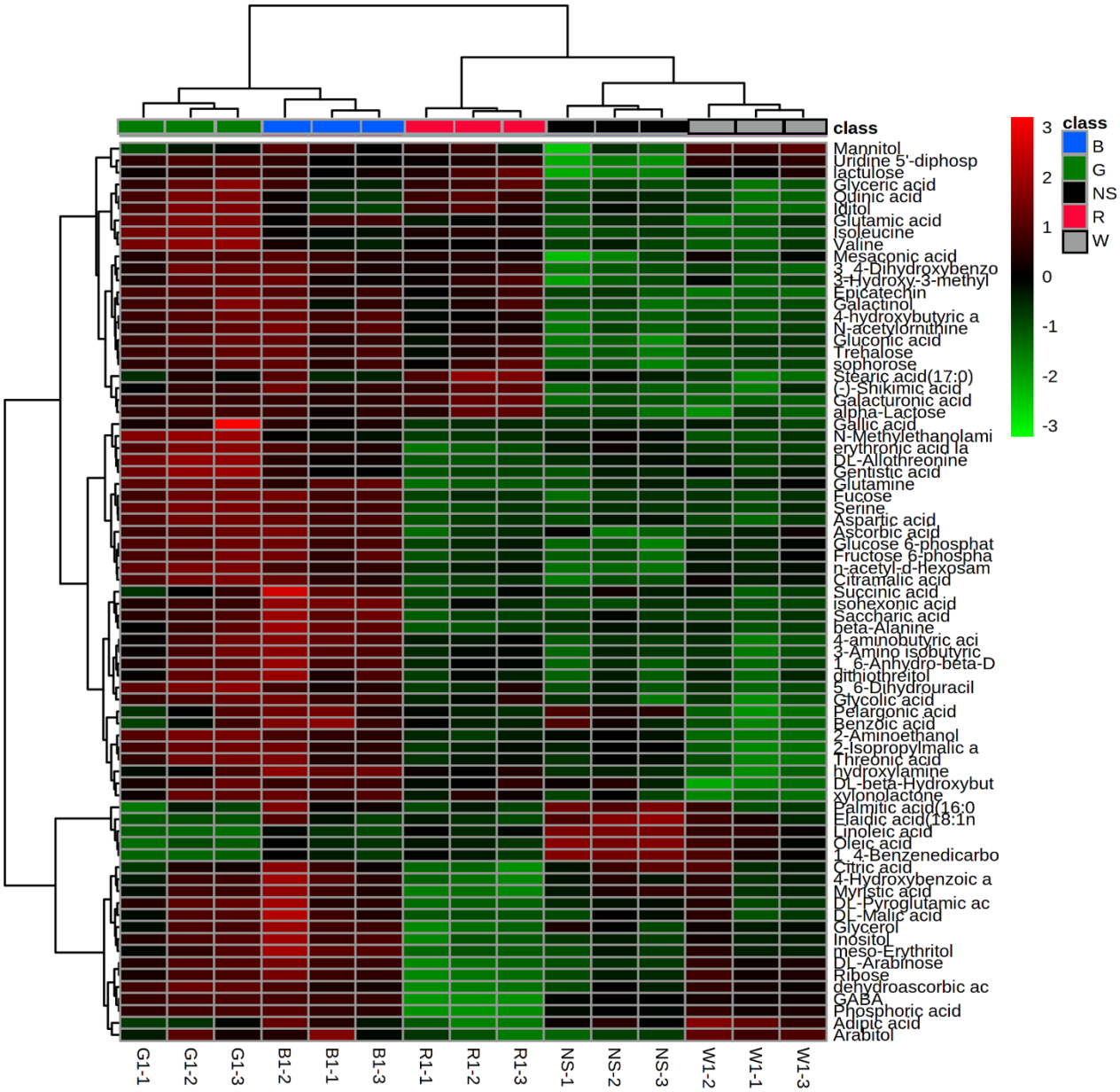
class
Mannitol
Uridine 5'-diphosp
lactulose
Glyceric acid
Quinic acid
Iditol
Glutamic acid
Isoleucine
Valine
Mesaconic acid
3_4-Dihydroxybenzo
3-Hydroxy-3-methyl
Epicatechin
Galactinol
4-hydroxybutyric a
N-acetylornithine
Gluconic acid
Trehalose
sophorose
Stearic acid(17:0)
(-)-Shikimic acid
Galacturonic acid
alpha-Lactose
Gallic acid
N-Methylethanolami
erythronic acid la
DL-Allothreonine
Gentistic acid
Glutamine
Fucose
Serine
Aspartic acid
Ascorbic acid
Glucose 6-phosphat
Fructose 6-phospha
n-acetyl-d-hexosam
Citramalic acid
Succinic acid
Isohexonic acid
Saccharic acid
beta-Alanine
4-aminobutyric aci
3-Amino isobutyric
1_6-Anhydro-beta-D
dithiothreitol
5_6-Dihydrouracil
Glycolic acid
Pelargonic acid
Benzoic acid
2-Aminoethanol
2-Isopropylmalic a
Threonic acid
hydroxylamine
DL-beta-Hydroxybut
xylonolactone
Palmitic acid(16:0
Elaidic acid(18:1n
Linoleic acid
Oleic acid
1_4-Benzenedicarbo
Citric acid
4-Hydroxybenzoic a
Myristic acid
DL-Pyroglutamic ac
DL-Malic acid
Glycerol
Inositol
meso-Erythritol
DL-Arabinose
Ribose
dehydroascorbic ac
GABA
Phosphoric acid
Adipic acid
Arabitol
G1-1
G1-2
G1-3
B1-2
B1-1
B1-3
R1-1
R1-2
R1-3
NS-1
NS-2
NS-3
W1-2
W1-1
W1-3
3
2
1
0
-1
-2
-3
class
B
G
NS
R
W

Fig. 4

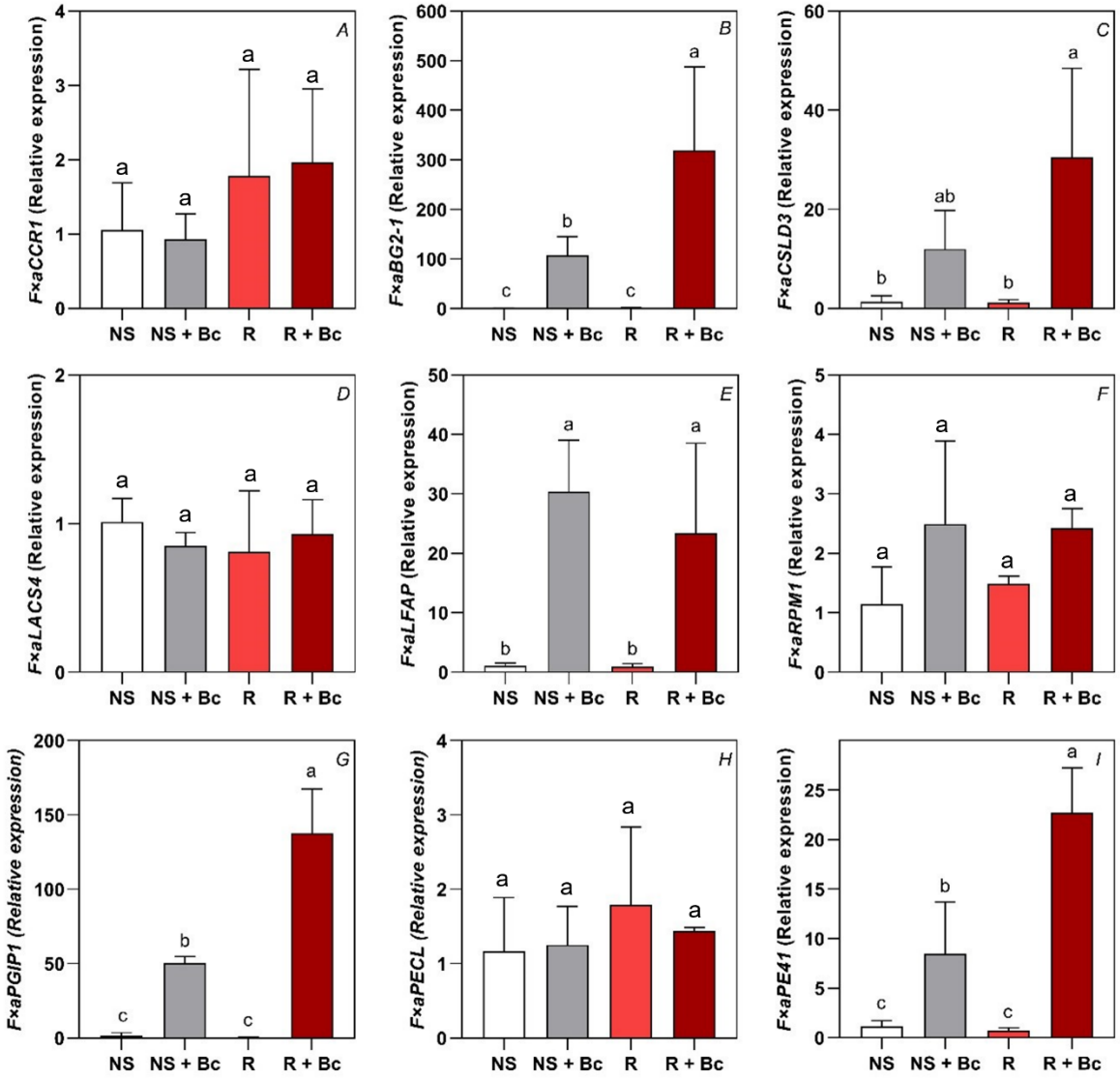
A
FxaCCR1 (Relative expression)
B
FxaBG2-1 (Relative expression)
C
FxaCSLD3 (Relative expression)
D
FxaLACS4 (Relative expression)
E
FxaLFAP (Relative expression)
F
FxaRPM1 (Relative expression)
G
FxaPGIP1 (Relative expression)
H
FxaPECL (Relative expression)
I
FxaPE41 (Relative expression)
NS
NS + Bc
R
R + Bc